



# Machine learning-based method for predicting C–V–T characteristics and electrical parameters of GaAs/AlGaAs multi-quantum wells Schottky diodes

Elyes Garoudja<sup>a,\*</sup>, Assia Baouta<sup>b</sup>, Abdeladhim Derbal<sup>b</sup>, Walid Filali<sup>a</sup>, Slimane Oussalah<sup>c</sup>, Meriem Khelladi<sup>b</sup>, Fouaz Lekoui<sup>d</sup>, Rachid Amrani<sup>e,f</sup>, Nouredine Sengouga<sup>g</sup>, Mohamed Henini<sup>h</sup>

<sup>a</sup> Plateforme Technologique de Micro-fabrication, Centre de Développement des Technologies Avancées, Cité 20 Aout 1956, Baba Hassen, Alger, Algeria

<sup>b</sup> Division Architecture des Systèmes et Multimédias, Centre de Développement des Technologies Avancées, Cité 20 Aout 1956, Baba Hassen, Alger, Algeria

<sup>c</sup> Division Microélectronique & Nanotechnologie, Centre de Développement des Technologies Avancées, Cité 20 Aout 1956, Baba Hassen, Alger, Algeria

<sup>d</sup> Division milieux ionisés & Laser, Centre de Développement des Technologies Avancées, Cité 20 Aout 1956, Baba Hassen, Alger, Algeria

<sup>e</sup> Département des sciences de la matière, Université Alger 1 Benyoucef Benkredda, Alger, Algeria

<sup>f</sup> LPCMME, Département de physique, Université d'Oran ES-Séria, Oran, Algeria

<sup>g</sup> Laboratory of Metallic and Semiconducting Materials, University of Biskra, BP 145 RP, 07000, Biskra, Algeria

<sup>h</sup> School of Physics and Astronomy, Nottingham Nanotechnology and Nano-Science Center, University of Nottingham, Nottingham, NG7 2RD, UK

## ARTICLE INFO

### Keywords:

Ant lion optimizer  
Multi-quantum wells  
Schottky barrier diode  
Capacitance-voltage characteristic  
Artificial neural network  
K-fold cross-validation

## ABSTRACT

In this work, two models of artificial neural networks are developed to predict the electrical parameters and capacitance-voltage characteristics of GaAs/AlGaAs multi-quantum wells Schottky diodes at different temperatures. Capacitance-Voltage-Temperature (C–V–T) characteristics for voltages and temperatures in the ranges (-4 V–0 V) and (20 K–400 K), respectively, were used to assess the effectiveness of the proposed approach. The first model (Model 1) is used to evaluate how well the neural network predicts the C–V–T characteristics. The second simulation, known as Model 2, was constructed to simultaneously overcome the problems of determining the electrical parameters and predicting C–V–T characteristics. Model 2 allows the calculation of the built-in voltage, effective density, and capacitance. Three-fold cross-validation and mean square error are used to assess the effectiveness of the developed models. The results clearly demonstrate the high prediction accuracy of the electrical parameters and C–V characteristics at all temperatures. After training, Model 1 Mean Square Error performance is  $1.5033 \times 10^{-6}$  at 1450 epochs, whereas Model 2 MSE is  $4.9951 \times 10^{-6}$  at 642 epochs. According to the error distribution frequency histogram, about 95 % of errors for Model 1 and Model 2 lie between [0.00535 and 0.005608] and [0.00328 and 0.00333], respectively. The R-values that correspond to the training and validation datasets for both models are close to one (0.9999). Parameters determination results have been compared against those obtained using ant lion optimizer based method. It was found that the results obtained from the neural networks models strongly agree with the experimental data.

## 1. Introduction

Schottky barrier diodes (SBDs) are crucial devices of many cutting-edge technical products owing to their distinctive electrical features [1]. They are employed as electrodynamic structures in a variety of applications, including optics, energy and health [2,3]. Characterization of SBDs are crucial since they could exhibit an important energy barrier during the metallization of semiconductor surfaces for external device connection [4]. High frequency and low power applications are dominated by III-V semiconductors (GaAs for instance) whereas silicon still

dominates microelectronics semiconductor industry [4]. Gates of metal-semiconductor field effect transistors (MESFETs) and high-electron mobility transistors (HEMTs) are made of III-V semiconductors-based Schottky contacts [4]. In addition, a variety of optoelectronic devices, including light-emitting diodes, lasers and photodetectors also utilize III-V semiconductors [5,6]. The efficiency of Schottky diodes may be enhanced by alloying various III-V semiconductors. To this aim, some complex structures including superlattices, quantum wells, quantum dots and quantum wires are employed [4]. Due to the high capacity of spanning a broad wavelength range [7],

\* Corresponding author. Plateforme Technologique de Micro-fabrication, Centre de Développement des Technologies Avancées, Baba Hassen, 16081, Alger, Algeria.

E-mail address: [egaroudja@cdta.dz](mailto:egaroudja@cdta.dz) (E. Garoudja).

GaAs/Al<sub>x</sub>Ga<sub>1-x</sub>As heterostructures are used to fabricate sophisticated detectors such as high sensitive bolometers [8].

Temperature dependence of current-voltage (I-V) and capacitance-voltage (C-V) characteristics may be used to study the thermal effects on the conduction mechanisms. Schottky diodes with an ideality factor equals to 1 are difficult to achieve for a variety of reasons, including non-ideal thermionic emissions, quantum mechanical tunneling and generation-recombination in the space charge region [4]. Therefore, the theoretical characteristics of ideal Schottky diodes are difficult to achieve, which assume an abrupt junction and fixed homogenous Schottky barrier height. This mismatch is considerably more pronounced in complicated structures like superlattices and multi-quantum wells (MQWs) [9]. Up to now, research that focuses on investigating the temperature dependence of I-V and C-V characteristics of SBDs is still ongoing [10–13]. Artificial neural network (ANN) techniques [14,15] may be used to address this issue. Indeed, to properly understand the electrical behavior of SBDs, a collection of synthetic data on I-V and C-V characteristics at different temperatures may be created using ANN model. Alade et al. [16] used the existing Sze and Monemar models to predict the change in breakdown voltage of n-type GaN Schottky diodes in the temperature range of 300–900 K. According to their findings, the breakdown voltage of n-type GaN Schottky diodes slowly drops with temperature increase. In order to determine the electrical characteristics of GaN Schottky diodes at high temperatures, Michael [17] employed a neural network based approach. In this work, microwave frequency sensors using GaN Schottky diodes were investigated, and the potential energy barrier height, depletion layer thickness and junction capacitance properties were estimated for the temperature range 300–950 K. Milosevic et al. [18] employed ANN to model the S-parameters of the SMS 7630 zero bias Schottky diodes. The measurements were obtained using a vector network analyzer with a frequency range of 0.5–5 GHz and an input power range –25 dBm to +5 dBm. The outcomes from the analysis of the learning and generalization capacities of the developed ANN were compared with experimental data. Darwish et al. [19] demonstrated the ability of enhancing the performance of Schottky diodes by using ANN system. The developed approach indicated that by optimizing temperature, current and voltage, the SBD performance may be improved. Çolak et al. [20] studied the effect of temperature on the I-V characteristics of Schottky diodes using ANN model. Current values were measured in the voltage range -2 V to +3 V at temperatures ranging from 100 K to 300 K. In this study, 362 experimental data were used to create a feed-forward back-propagation ANN to estimate the diode I-V characteristics at different temperatures. The ANN outputs were found to be very consistent with the experimental Schottky diode data. The results showed that ANN is a good model for predicting the temperature-dependent current-voltage characteristics of Schottky diodes. Güzel et al. [1] developed an ANN model to estimate the current values of a 6H-SiC/MEH-PPV Schottky diode with polymer interface. Training stage was achieved using experimentally recorded current values between 100 K and 250 K and -3 V to +3 V. The results showed that ANNs are excellent approaches for determining the I-V characteristics of a polymer-interfaced 6H-SiC/MEH-PPV Schottky diode at various temperatures. Güzel et al. [21] proposed an experimental study of the aptitude of ANN to predict the capacitance values of the polymer-interface 6H-SiC/MEH-PPV/Al Schottky diodes at different frequencies. 480 experimental data points were used in the training of the feed-forward back-propagation network model with five neurons per hidden layer. The network model's prediction was tested by comparing the experimental data with the estimated values of ANN. Çolak et al. [22] suggested three different ANN simulations to evaluate the capacitance-voltage characteristics of a Schottky diode with an organic polymer edge that is frequency dependent. Levenberg–Marquardt (LM) method was employed during the training stage of the developed Multilayer Perceptron (MLP) networks that incorporated 5, 10, and 15 neurons in the hidden layers. The obtained results showed that the developed ANN structures exhibit excessive deviations and are unable to

estimate the frequency-dependent capacitance-voltage characteristics of the organic polymer interface Schottky diodes.

The usefulness of machine learning approach in determining the Schottky diodes electrical parameters has been examined by Güzel et al. [23]. The developed MLP model was constructed using 368 data sets, and its hidden layer determined the values of voltage and temperature, while the output layer computed the current values. With an average variance of 0.11 %, the neural network model that was created was able to predict the electrical characteristics of Schottky diodes. The prediction of I-V characteristics at low temperatures was examined by using an ANN model trained on high temperature data [24]. Experimental I-V characteristics between 80 and 375 K were used to develop the model. Temperature and voltage were defined as input parameters of the network, while the current was the output parameter. It is important to point out that all studies reported in the literature provide remarkable prediction performance using ANNs.

Many researchers [4,10,13,25,26] were also interested in investigating the thermal effects on the electrical parameters of SBDs, including the ideality factor, barrier height, series resistance, saturation current, carrier effective density and built-in voltage. Heuristics and analytical techniques can both be used to determine the diode parameters. When using heuristic techniques, the parameter determination step is viewed as an optimization problem where a cost function is defined and mathematically optimized [27]. Several heuristics algorithms were employed to address this issue, including artificial bee colony (ABC) [28], best-so-far ABC [29], particle swarm optimization (PSO) [30], differential evolution (DE) [31], dragonfly algorithm (DA) [32] and antlion optimizer (ALO) [33].

Filali et al. [10] suggested an effective parameter determination method for C-V-T characteristics of a MQW diode using the ALO algorithm. The efficiency of this strategy was assessed through experimentation after fabricating and characterizing the diodes. The investigation of temperature effect on the Be-doped Al<sub>0.29</sub>Ga<sub>0.71</sub>As Schottky diode parameters has also been reported by Filali et al. [11]. This work addressed the diode parameter determination step as a mathematical optimization issue that was solved using DA technique. Garoudja et al. [12] conducted a comparative analysis of several approaches for deriving MQW diode parameters using I-V characteristics. In their study, PSO, DE, and ABC algorithms were used to deal with the parameter determination stage, while the Cheung technique was chosen as an analytical extraction approach. The high efficiency of heuristics algorithms in accurately determining the diodes' parameters is clearly evidenced from the analysis of the above works.

On the other hand, analytical strategies such as I-V [34], Cheung and Cheung [25] and Norde [35] methods have also been employed. However, they are utilized only within a limited voltage range. Oussalah et al. [13] investigated the I-V-T properties of Be-doped AlGaAs Schottky diodes grown on (100) GaAs substrates using molecular beam epitaxy. This study examined the effect of temperature on the electrical characteristics of diodes at temperatures ranging from 260 to 400 K.

The main contribution of this work is to address the lack of research on using ANNs and heuristics algorithms to predict C-V characteristics and diode electrical parameters simultaneously. Indeed, characteristics prediction and parameters determination have always been addressed separately. Moreover, the efficiency test of our approach was done using experimental data obtained at different conditions (from low to high temperatures). For the test, we began by training the network using C-V data acquired at specified temperatures and attempting to accurately predict results at others temperatures never seen by the network. In this study the network is also trained with some data of the same temperature and then evaluate its ability to anticipate the other points of the C-V characteristics as well as the diode's electrical parameters at the same temperature. In this work, for the first time, an efficient ANN model has been developed to deal with this issue. The effectiveness of the developed model was evaluated using experimental C-V data obtained in the temperature range 20–400 K. Moreover, the estimated electrical

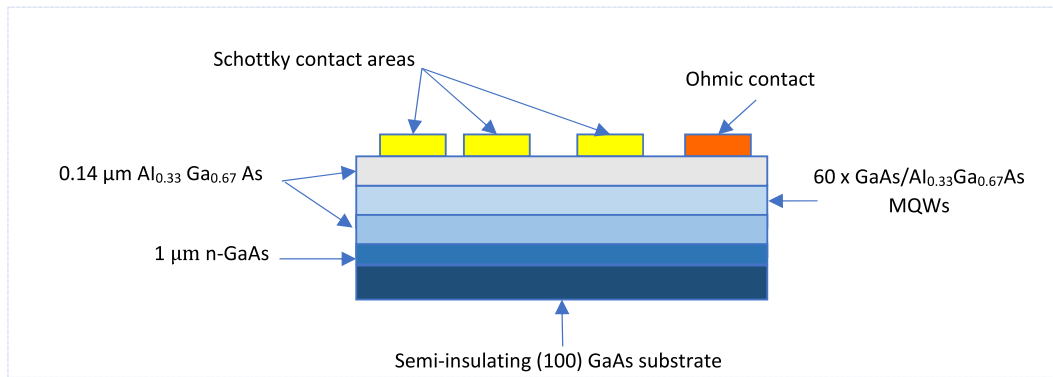


**Fig. 1.** Schematic diagram of the fabricated Schottky diodes.

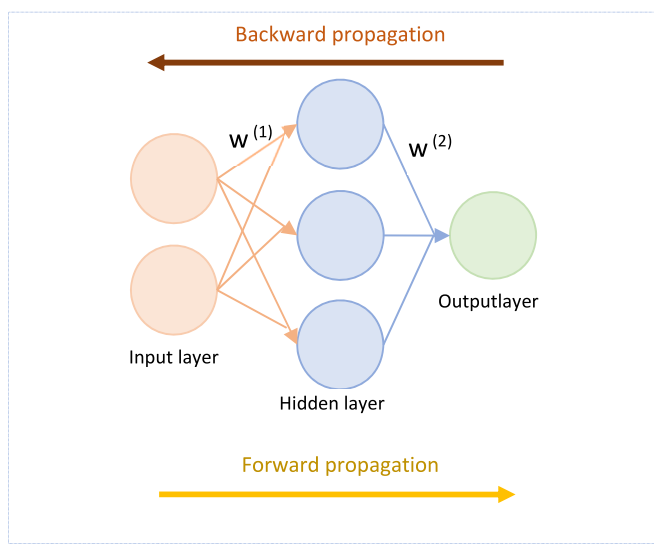


**Fig. 2.** Artificial neural network architecture with one hidden layer.

parameters, which were obtained using the developed ANN, are compared with those acquired using ALO-based heuristic method [10]. The observed results prove the high efficiency of ANN model in both electrical characteristics prediction and parameters determination.

## 2. Experimental

The n-type silicon-doped MQW Schottky diode structure investigated in this study, namely NU1054, was grown at Nottingham University on a semi-insulating (100) GaAs substrate using molecular beam epitaxy (MBE) technique [4]. The layer structure consists of (i) semi-insulating (100) GaAs substrate, (ii) 1 μm Si-doped GaAs buffer layer, (iii) 0.14 μm n-type Al<sub>0.33</sub>Ga<sub>0.67</sub>As barrier, (iv) 60 periods of 50 Å n-type GaAs/89 Å n-type Al<sub>0.33</sub>Ga<sub>0.67</sub>As MQWs, (v) 0.14 μm n-type Al<sub>0.33</sub>Ga<sub>0.67</sub>As. The doping concentrations of GaAs and Al<sub>0.33</sub>Ga<sub>0.67</sub>As layers were  $2 \times 10^{16}$  cm<sup>-3</sup> and  $1.33 \times 10^{16}$  cm<sup>-3</sup>, respectively. The growth of the structure was carried out at substrate temperature of 630 °C.

Ohmic contact was formed by evaporating layers of Ge/Au/Ni/Au and then performing a thermal anneal at 360 °C for 30 s. Schottky contacts were obtained by evaporating Ti/Au at 410 °C on top of the n-type Al<sub>0.33</sub>Ga<sub>0.67</sub>As layer (Fig. 1).

## 3. Methodology

This paper consists on the development of a new approach based on ANN to predict C-V characteristics and determine the electrical

parameters of SBDs at low and high temperatures. To reach this goal, the following subsections give details about ANN and parameters determination approach using ALO algorithm.

### 3.1. Artificial neural network

An artificial neural network (ANN) [15] is a computer representation of how nerve cells function in human brain. ANNs make use of learning methods that enable them to autonomously modify their responses using fresh data. For non-linear data modeling, they are therefore a particularly powerful tool [14]. There are three or more linked layers in an ANN (Fig. 2). Neurons in the input layer make up the first layer. These neurons transmit information to the deeper layers (hidden layers), which then transmit the final output information to the output layer. ANNs consist of forward propagation and backward propagation.

Computation and storing of intermediate variables (including outputs) for a neural network in a proper sequence from the input layer to the output layer is referred to as forward propagation. Indeed, a collection of weights described as two-dimensional matrices  $w_{ij}$  connects one or more hidden levels to the exterior layers. The value of each node is the output  $y_i$  (Eq. (1)) [36] of a nonlinear activation function  $f$  whose argument is the weighted sum over all the nodes in the preceding layer plus a constant component  $b_0$ , referred to as the bias.

$$y_i = f(z_i) = f\left(\sum_j w_{ij}x_j + b_0\right) \quad (1)$$

There are several types of activation functions, denoted by  $f$ . For example, the threshold function (Eq. (2)) [36] which takes on a value of 0 or 1 if the summed input is less or more than a certain threshold value ( $v$ ), respectively.

$$f = \begin{cases} 1 & \text{if } z_i \geq v \\ 0 & \text{if } z_i < v \end{cases} \quad (2)$$

Another activation function is the Sigmoid one, which can range between 0 and 1. An example of the sigmoid function is the hyperbolic tangent function (Eq. (3)) [37].

$$f(z_i) = \tanh\left(\frac{z_i}{2}\right) = \frac{1 - \exp(-z_i)}{1 + \exp(-z_i)} \quad (3)$$

The foundation of neural net training is backward propagation. It is the process of adjusting a neural network's weights depending on the error rate (also known as loss) realized in the preceding epoch (also known as iteration). Lower error rates are ensured by proper weight adjustment [15].

The topology of a neural network is determined by a large number of variables known as hyperparameters. These variables determine how the network structure is trained. The hyperparameters are chosen before optimizing the network's biases and weights. Here is a list of the most

**Table 1**

List of used hyperparameters for both Models.

	Model 1	Model 2
Number of hidden layers	02	02
Number of neuron in hidden layers	03/02	04/03
Activation function of hidden layer	Tansig	Tansig
Activation function of output layer	Purelin	Purelin
Number of epochs	3000	3000
loss function	Mean square error	Mean square error
Initialization strategy	random	Random
Training algorithm	Levenberg–Marquardt	Levenberg–Marquardt

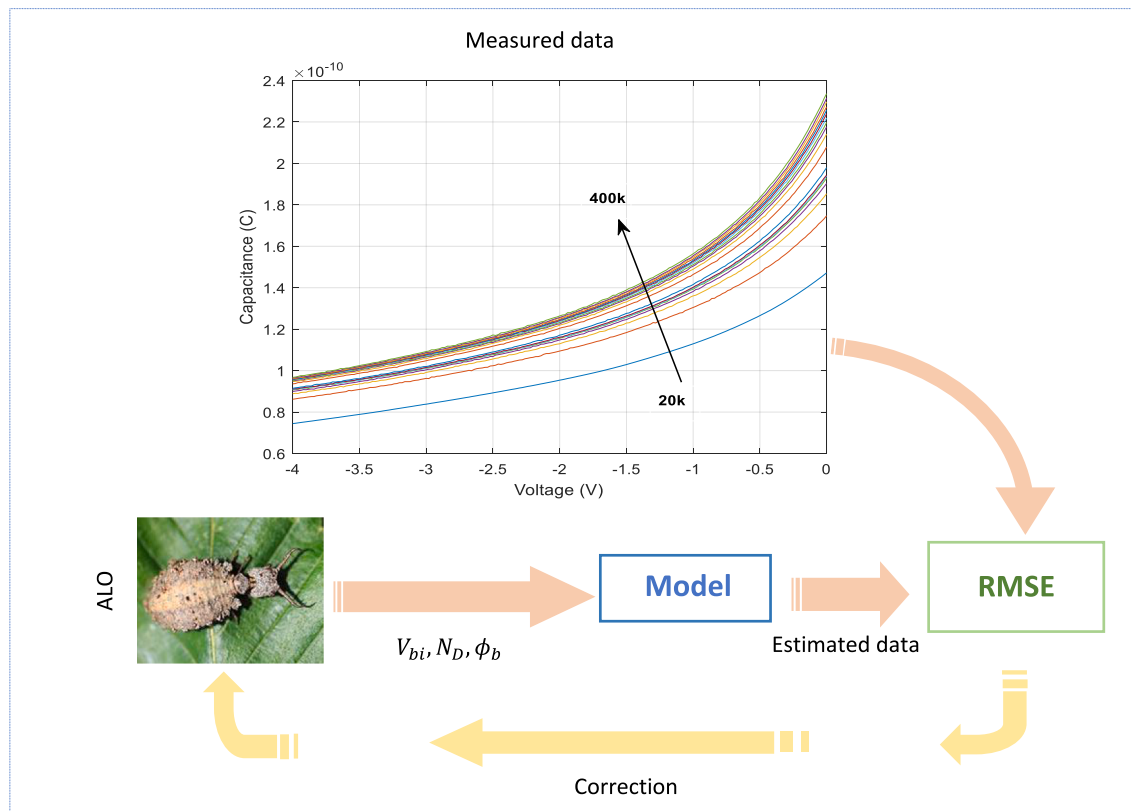
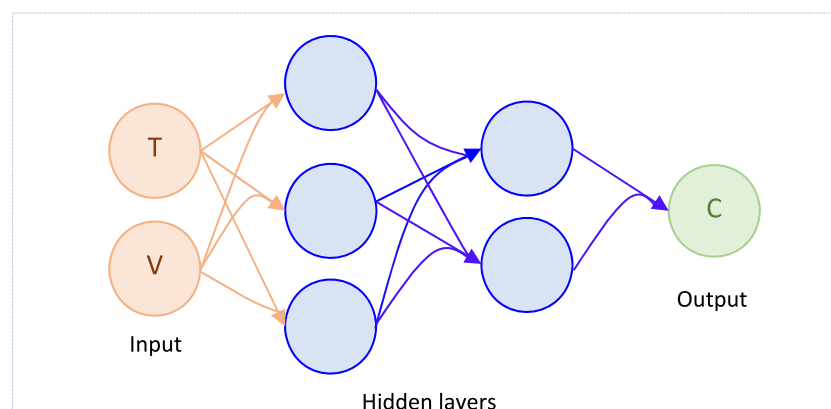
relevant hyperparameters with the appropriate descriptions [38].

- The activation function: it determines whether a neuron should be activated or not by computing the weighted sum and then applying bias to it. The activation function's objective is to add nonlinearity to a neuron's output.
- Layers number: called also number of hidden layers, which is the number of layers between input and output layers.

**Table 2**

List of temperatures used for training and testing Model 1.

Training temperatures (K)	Testing temperatures (K)
20, 40, 80, 120, 160, 200, 240, 280, 320, 360, 400	60, 100, 140, 180, 220, 260, 300, 340, 380

**Fig. 3.** ALO-based approach to determine the SBD electrical parameters.**Fig. 4.** Schematic diagram of Model 1.

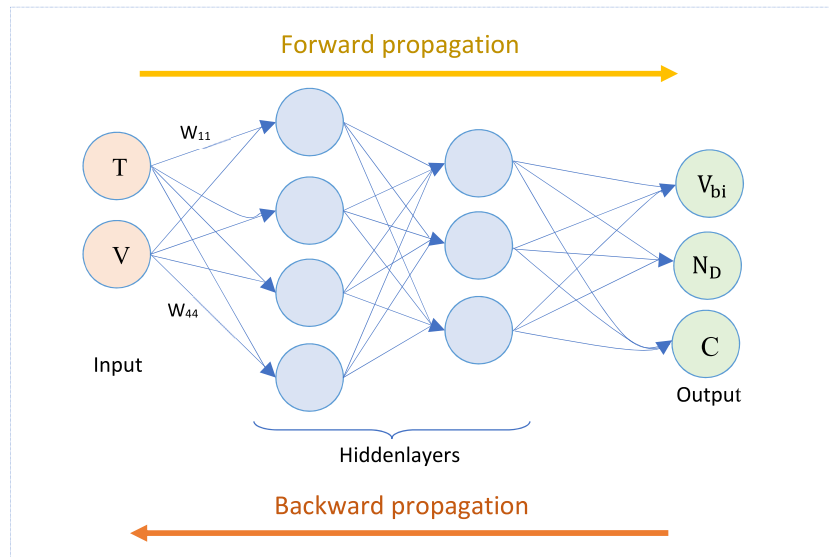


Fig. 5. Schematic diagram of Model 2.

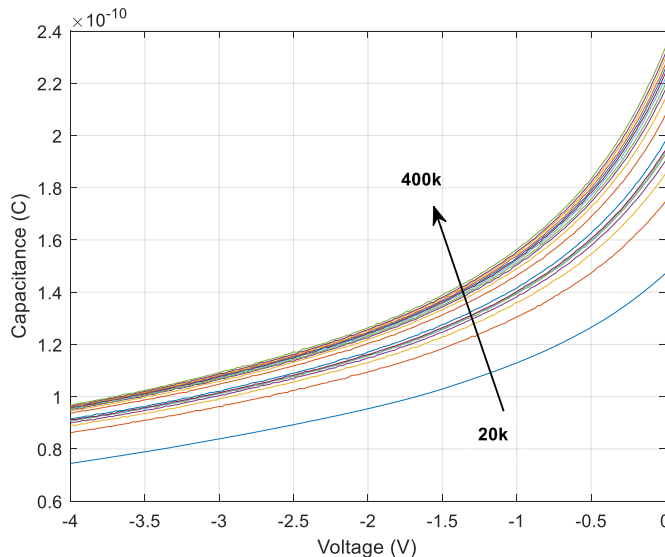


Fig. 6. Measured C-V characteristics of Schottky diode for different temperatures.

- Number of neurons in each layer.
- The number of epochs: it refers to how many times all training examples were passed through the network during training.
- Learning rate: Gradient Descent (GD) is a fundamental optimization process used in machine learning to minimize a cost function and get the best values for model parameters. The learning rate ( $\alpha$ ) determines how soon the algorithm converges to the minimum of the cost function. It effectively determines the step size used in each iteration of the gradient descent process. It should be noted that with a small learning rate, the gradient descent technique requires more iterations to reach the minimum, resulting in slower convergence. However, with a high learning rate, the algorithm moves quickly toward the minimum, but it may constantly overshoot, causing the cost function to increase rather than decrease. This can result in divergence, where the algorithm fails to identify the best solution and instead moves away from it.

- The loss function: it specifies how to compute the error between prediction and label for a particular training sample. During training, the error is backpropagated to update both weights and bias.
- Loss function regularization: it is a penalty component added to the gradient update equation or loss function to prevent overfitting and/or make the network robust to the noisy input data.
- Initialization strategies for learnable parameters: before beginning the training stage, the learnable parameters (as weights and bias) of neurons must be assigned with starting values. These values can influence the complexity of the learning task by varying the probabilities of meeting local minima.

On the other hand, ANN parameters learned via the GD method are changed in backpropagation during the training. The parameters are weights and bias.

Several ways have been offered in the literature to handle the hyperparameter selection problem. The following approaches have been adopted [38].

- Grid search: Complete Manual and Random: it involves evaluating the loss for each possible configuration of the hyperparameters in order to identify the lowest loss. Because all possible configurations must be evaluated, conducting a comprehensive grid search is time-consuming. As a result, a subset of configurations can be chosen manually using intuition before or during the grid search process. However, this poses repeatability issues and requires hyperparameter adjustment to be conducted sequentially. The most used type of grid search is random grid search, which selects parameter combinations at random.
- Bayesian Optimization: in recent years, this type of approach has gained popularity for ANN hyperparameters optimization (HPO). One of the main reasons for creating Bayesian ANN HPO is that evaluating the loss function is quite costly since it requires complete retraining of the ANN for each hyperparameter configuration.
- Population-based Method: in this type of method, the network best configuration may be viewed as the result of having several architectural candidates competing for the best fitness in an environment with limited resources and many constraints (data). For example, PSO and Genetic Algorithm (GA) are well-known population-based optimization techniques that are often used to optimize weights and bias initialization stages prior to the GD establishment [39,40].

On the basis of the aforementioned details, it should be noted that a

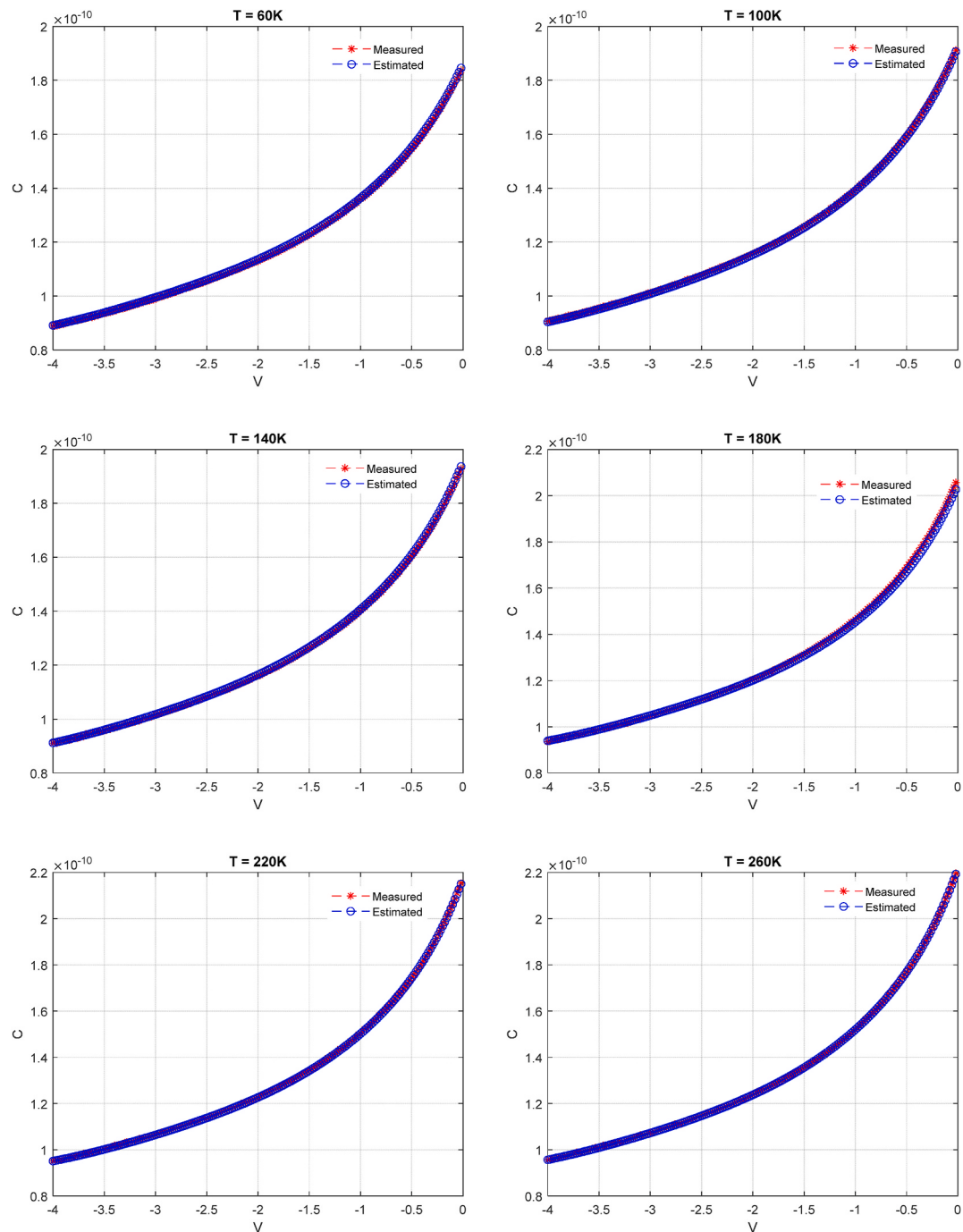


**Fig. 7.** Measured and predicted C-V characteristics of the testing set at temperatures: 60, 100, 140, 180, 220, 260, 300, 340, and 380 K.

complete grid search strategy to select the optimal values of those hyperparameters have been employed in this work. In other words, several possible configurations have been verified until the best results are obtained. The list of the used hyperparameters is summarized in Table 1. Where, the activation functions are given by equations (4) and (5) [22]:

$$Tansig(x) = \frac{1}{1 + e^{-x}} \quad (4)$$

$$purelin(x) = x \quad (5)$$

The amount of error between the predicted values of the ANN model and the target values was also examined. The formulas that are used to

calculate the performance parameters are given by equations (6) and (7) [22]:

$$MSE = \frac{1}{N} \sum_{i=1}^N (X_{measured(i)} - X_{estimated(i)})^2 \quad (6)$$

$$R = \sqrt{1 - \frac{\sum_{i=1}^N (X_{measured(i)} - X_{estimated(i)})^2}{\sum_{i=1}^N (X_{measured(i)})^2}} \quad (7)$$

where  $X_{measured(i)}$  and  $X_{estimated(i)}$  are measured and ANN-based estimated values, respectively.

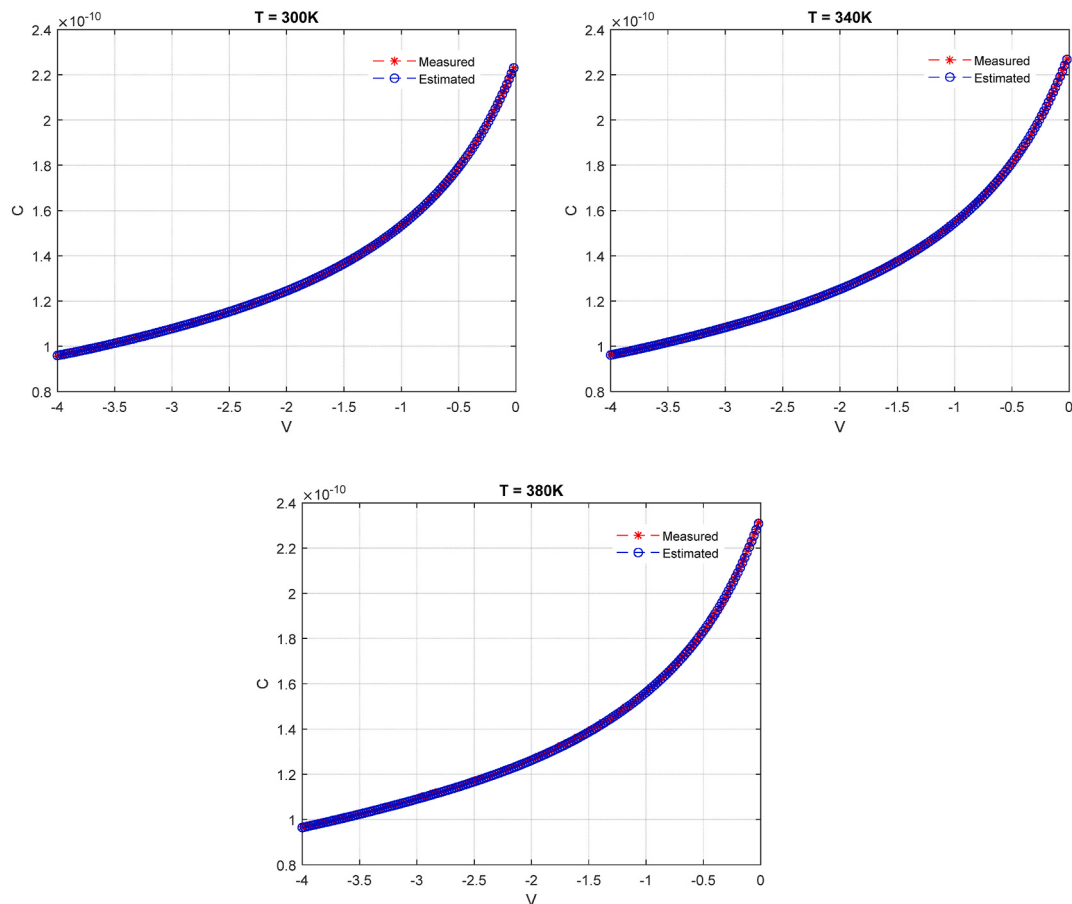


Fig. 7. (continued).

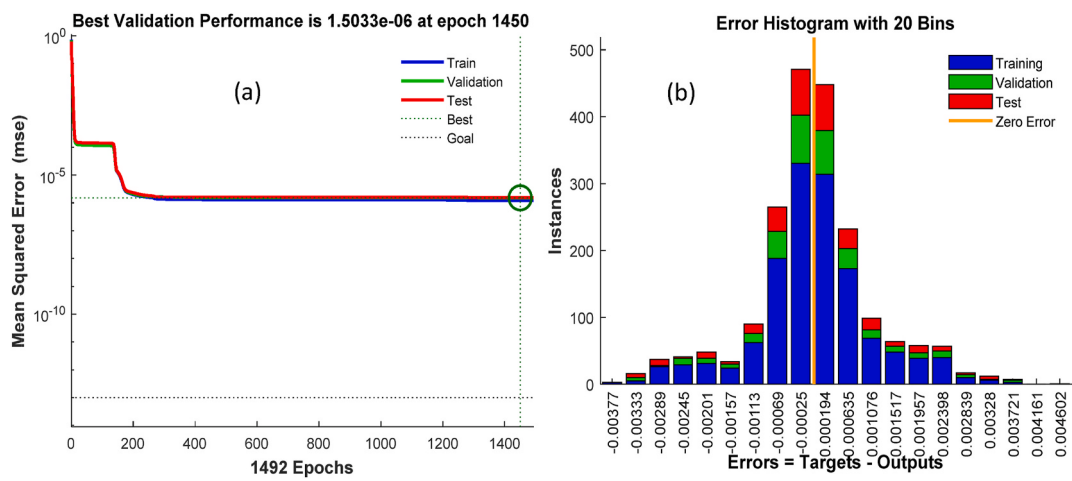


Fig. 8. (a) Training performance of Model 1 according to epoch. (b) Error histogram of Model 1.

### 3.2. Diode parameters determination

The capacitance-voltage (C-V) characteristic represents the electrical behavior of a Schottky diode as given by equation (8) [10,34]:

$$\frac{C}{A} = \sqrt{\frac{\mp qeN_{eff}}{2\left(\mp V_{bi} \mp V - \frac{kT}{q}\right)}} \quad (8)$$

where  $A$  is the contact area ( $1.13 \times 10^{-2} \text{ cm}^{-2}$ ),  $q$  is the electron charge

$(-1.602 \times 10^{-19} \text{ C})$ ,  $\epsilon$  is the AlGaAs permittivity ( $8.94 \times 10^{-11}$ ),  $N_{eff}$  is the effective density of the carriers and  $V_{bi}$  is the built-in voltage. The (+) and (-) signs relate to p-type and n-type semiconductors, respectively. The diode capacitance and operating voltage are denoted as  $C$  and  $V$ , respectively.

Since the foundation of this study is an n-type Schottky diode, the Schottky barrier height  $\Phi_b$  may be calculated as [10,34]:

$$\Phi_b = V_{bi} + \frac{KT}{q} \ln \left( \frac{N_c}{N_D} \right) \quad (9)$$

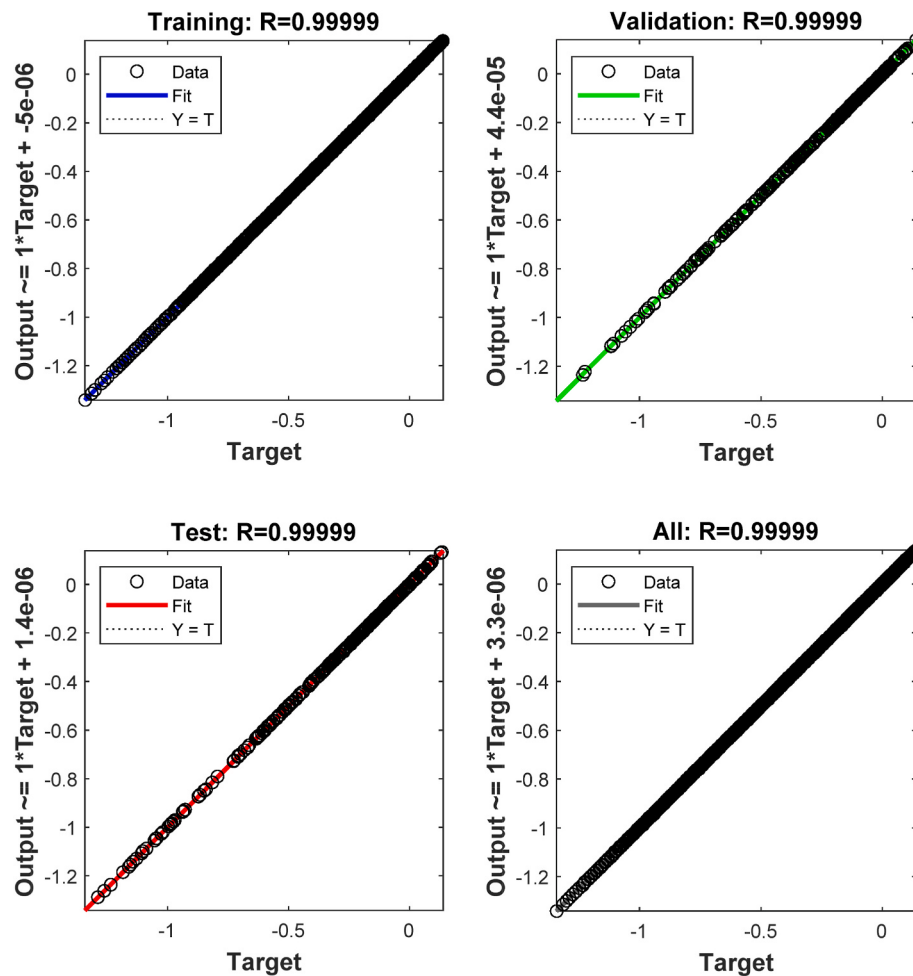


**Fig. 9.** The R-values calculated for training, validation, test and all data sets of Model 1.

**Table 3**

Results of Schottky diode parameters determination using Model 2 and ALO-based method.

Temperature (K)	Built-in voltage (V)		Effective density ( $\text{cm}^{-3}$ )	
	Model 2	ALO	Model 2	ALO
20	1.444	1.4439	$3.16 \times 10^{15}$	$3.1598 \times 10^{15}$
40	1.3294	1.3293	$4.0378 \times 10^{15}$	$4.0376 \times 10^{15}$
60	1.2196	1.2191	$4.173 \times 10^{15}$	$4.174 \times 10^{15}$
80	1.1778	1.1784	$4.23 \times 10^{15}$	$4.228 \times 10^{15}$
100	1.1658	1.1655	$4.2693 \times 10^{15}$	$4.2714 \times 10^{15}$
120	1.15	1.1493	$4.28 \times 10^{15}$	$4.275 \times 10^{15}$
140	1.144	1.146	$4.282 \times 10^{15}$	$4.29 \times 10^{15}$
160	1.127	1.126	$4.32 \times 10^{15}$	$4.31 \times 10^{15}$
180	1.047	1.049	$4.438 \times 10^{15}$	$4.451 \times 10^{15}$
200	0.997	0.996	$4.498 \times 10^{15}$	$4.49 \times 10^{15}$
220	0.973	0.971	$4.518 \times 10^{15}$	$4.515 \times 10^{15}$
240	0.956	0.957	$4.527 \times 10^{15}$	$4.525 \times 10^{15}$
260	0.942	0.942	$4.533 \times 10^{15}$	$4.538 \times 10^{15}$
280	0.929	0.928	$4.538 \times 10^{15}$	$4.541 \times 10^{15}$
300	0.916	0.916	$4.541 \times 10^{15}$	$4.543 \times 10^{15}$
320	0.903	0.904	$4.546 \times 10^{15}$	$4.547 \times 10^{15}$
340	0.891	0.891	$4.543 \times 10^{15}$	$4.546 \times 10^{15}$
360	0.88	0.879	$4.565 \times 10^{15}$	$4.561 \times 10^{15}$
380	0.868	0.869	$4.583 \times 10^{15}$	$4.591 \times 10^{15}$
400	0.858	0.858	$4.606 \times 10^{15}$	$4.603 \times 10^{15}$

where  $N_c = 1.11 \times 10^{16} \text{ cm}^{-3}$  is the effective density of states in the conduction band for  $\text{Al}_{0.33}\text{Ga}_{0.67}\text{As}$  and  $N_D$  is donor density (because of n-type Schottky diode).

Authors recently suggested an efficient heuristic-based method [10] to determine  $V_{bi}$ ,  $N_D$ , and  $\Phi_b$ . It employs the antlion optimizer (ALO) algorithm [33,41]. ALO is based on antlions natural hunting mechanism. The five fundamental stages of hunting prey employed by ALO are (i) the random movement of ants, (ii) traps construction, (iii) the entrapment of ants, (iv) the gathering of preys and (v) the re-building of traps [41]. Detailed description about ALO algorithm is given in Ref. [41]. ALO is used to find the electrical parameters of the diode by considering this stage as a mathematical optimization problem. The cost function to be optimized (minimized in this case) is defined as the Root Mean Square Error (RMSE) between measured and estimated C-V characteristics. The following diagram (Fig. 3) depicts the main stages of ALO-based parameter determination approach [10].

More details about the developed strategy based on ALO to determine the SBD electrical parameters, are given in Ref. [10].

### 3.3. Proposed approach

The main contribution of this work is the elaboration of an ANN model that can at the same time predict the C-V characteristics and determine the diode electrical parameters. To reach this goal, the aptitude of ANN to accurately predict C-V characteristics at different temperatures should firstly be tested without taking into account the parameters determination stage. A feed-forward back-propagation ANN model, named Model 1, with two hidden layers was developed to deal with this issue. Experimental C-V characteristics obtained from the electrical characterization of the elaborated sample are used to train and test Model 1. Fig. 4 shows that Model 1 has two inputs (temperature and

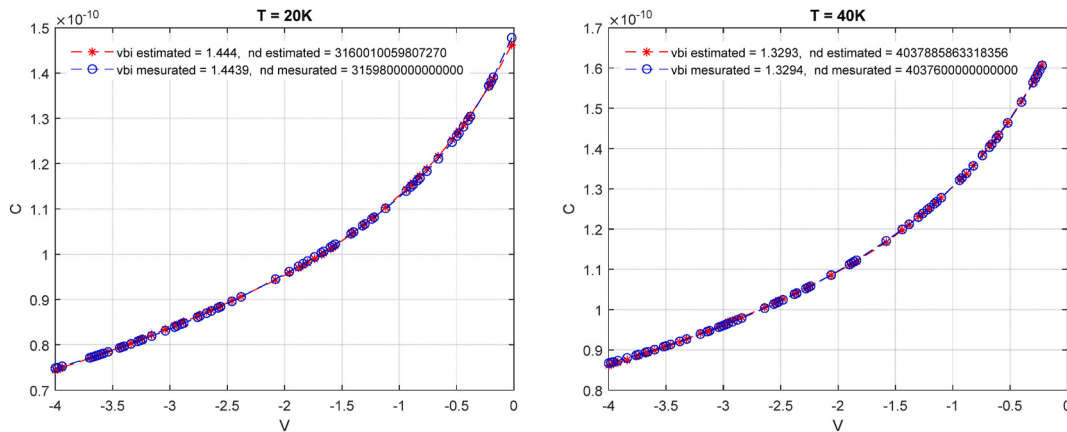


**Fig. 10.** The C–V characteristics for calculated (by ALO) and estimated (by Model 2) parameters at different temperatures.

voltage) and one output (capacitance). It consists of two neurons in the input layer, two hidden layers that contain three and two neurons, respectively, and one neuron in the output layer. This choice of number of layers and neurons in each layer was done after having tested Model 1 for different configurations and then the best one was selected. Mean square error (MSE) is used to evaluate Model 1. Temperatures used for the training and testing of Model 1 are displayed in Table 2. Temperature selection process for the training and testing stages was done at random.

The utilized database contains.

- 800 samples of voltage (20 vectors of 40 samples each); Voltage values ranged from –4 to 0 V with a sample step of 0.1 V.
- 800 samples of temperature (20 vectors of 40 samples each); Temperatures spanning the range of 20–400 K with a sample step of 20 °C
- 800 samples of capacitance (20 vectors of 40 samples each)

After having successfully checked the efficiency of Model 1 (C–V prediction), its capacity to predict at the same time C–V characteristic and determine the electrical parameters ( $V_{bi}$ ,  $N_D$ ,  $\Phi_b$ ) is assessed. An ANN model labeled Model 2 (Fig. 5) has been built to address this issue. Fig. 5 shows that Model 2 includes one input layer with two neurons, two hidden layers with four and three neurons, and one output layer with three neurons. The same criteria used for Model 1 are used to determine the number of layers and neurons in each layer for Model 2. It features two inputs (temperature and voltage) and three outputs ( $V_{bi}$ ,  $N_D$ ,  $C$ ). MSE and 3-fold cross-validation are used to evaluate Model 2, as follows [42]:

- Shuffle the entire dataset in a random manner.
- Split the entire dataset into 3 groups.

For each group:

- Consider this group as the testing set.
- Consider the remaining two groups as the training set.
- Train Model 2 using the training set and evaluate it using the testing set.
- Store the evaluation score (MSE value).
- Select the best configuration (best tuned biases and weights) based on the obtained scores of each group.

#### 4. Results and discussion

Fig. 6 shows the experimental C–V characteristics of the elaborated

diode (NU1054), which will then be employed in Models establishment. DLTS characterization system at Nottingham University was used to elaborate this stage [4]. A usual C–V behavior, where the capacitance value increases with temperature at reverse bias, can be observed by analyzing the measured characteristics.

This is mostly a result of the carriers' accumulation phenomena. Additionally, the acquired C–V characteristics at high and low temperatures (20 and 400 K) served as evidence for the reliability of Schottky diodes.

The first goal is to develop Model 1, which serves to predict the C–V characteristics at different temperatures. To address this issue, as described in the earlier section, characterization findings are used. The parameters of Model 1 (as synaptic weights and biases) are tuned once it has been trained with adequate data (as seen in Table 2). The testing data is then fed into Model 1 (which has already been trained), and a comparison between the expected and actual results is performed. The outcomes achieved using the test data on the already trained network (Model 1) are shown in Fig. 7. The outcomes strongly show how well Model 1 can predict the C–V characteristic across all test temperatures.

The MSE variation for training, validation, and testing is shown in Fig. 8 (a). The performance after training has an MSE of  $1.19 \times 10^{-6}$  at 1492 epochs, whereas the best validation performance is  $1.5033 \times 10^{-6}$  at 1450 epochs. Training was halted at the 1450th epoch since the validation error was at its lowest value. Utilizing the adjusted weights and biases, the modeling was then completed.

The frequency histogram of error distribution is depicted in Fig. 8 (b). The peak value of the error distribution histogram is around 0.00025 (absolute value), meaning that the majority of the errors are close to zero. Furthermore, nearly 95% of error fall between 0.00328 and 0.00333.

The outputs of Model 1 were then subjected to linear regression in order to compare them to the actual data (measurements). In an ideal model, all data points would be situated on the diagonal line of the correlation graph, which is the case of this study. Fig. 9 shows that for the training, testing and validation sets, as well as the entire data set, there is a significant correlation between estimated and expected values. The R-values for the three data sets (training, validation, and testing) are close to one (0.9999). Furthermore, for the training, validation, and testing data sets, the slopes of regression lines are all equal to 1 and their intercepts are all very close to zero ( $-5 \times 10^{-6}$ ,  $4.4 \times 10^{-5}$  and  $1.4 \times 10^{-6}$ , respectively).

The next stage is to develop Model 2 and assess its effectiveness in predicting the C–V characteristics and determining the diode electrical parameters. Therefore, it is necessary to employ the already determined electrical parameters based on ALO algorithm. Table 3 lists the results of NU1054 parameters determination using ALO, which were recently

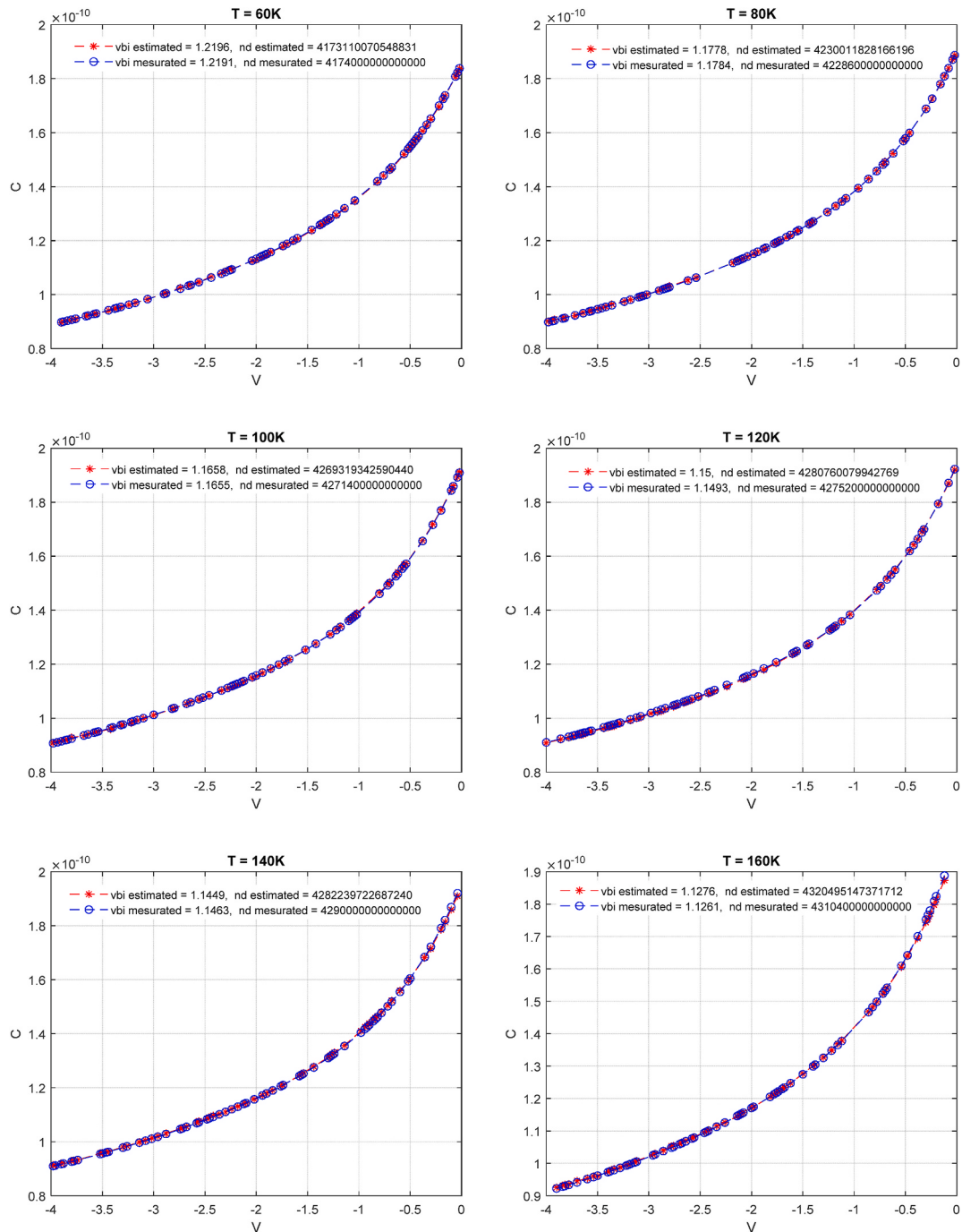


Fig. 10. (continued).

published in Ref. [10]. It should be noted that ALO-based approach was used to determine  $V_{bi}$  and  $N_d$ , while  $\Phi_b$  values have been computed using Equation (9).

The findings of parameters determination using the ALO-based approach and those derived using Model 2 are displayed in Table 3.

Results in Table 3 clearly demonstrate a good similarity between results produced using Model 2 and those acquired using the ALO-based technique for all temperatures. Furthermore, the plot of measured and predicted C-V characteristics (Fig. 10) of the testing data set has been used to assess the prediction capacity of Model 2. It can be clearly observed that for all temperatures, there is a good fit and agreement between the estimated and measured C-V characteristics.

Fig. 11(a) shows the MSE variation for training, validation, and

testing of Model 2. The performance after training has an  $MSE = 5.81 \times 10^{-6}$  at 842 epochs, whereas the best validation performance is  $4.9951 \times 10^{-6}$  at 642 epochs. The modeling was terminated, and the optimized weights and biases were saved once the training was done at the 1450th epoch (the lowest validation error was reached).

Fig. 11(b) displays the error distribution's frequency histogram. Most of the errors are very close to zero since the peak is close to 0.00097. Additionally, between 0.00535 and 0.005608, Errors were present in over 95 % of the instances.

The outputs of Model 2 were then compared to the actual measured data using linear regressions, as shown in Fig. 12. It can be seen that similarly to the results of Model 1, the diagonal of the correlation graph is the location of all the data points. Moreover, a significant connection

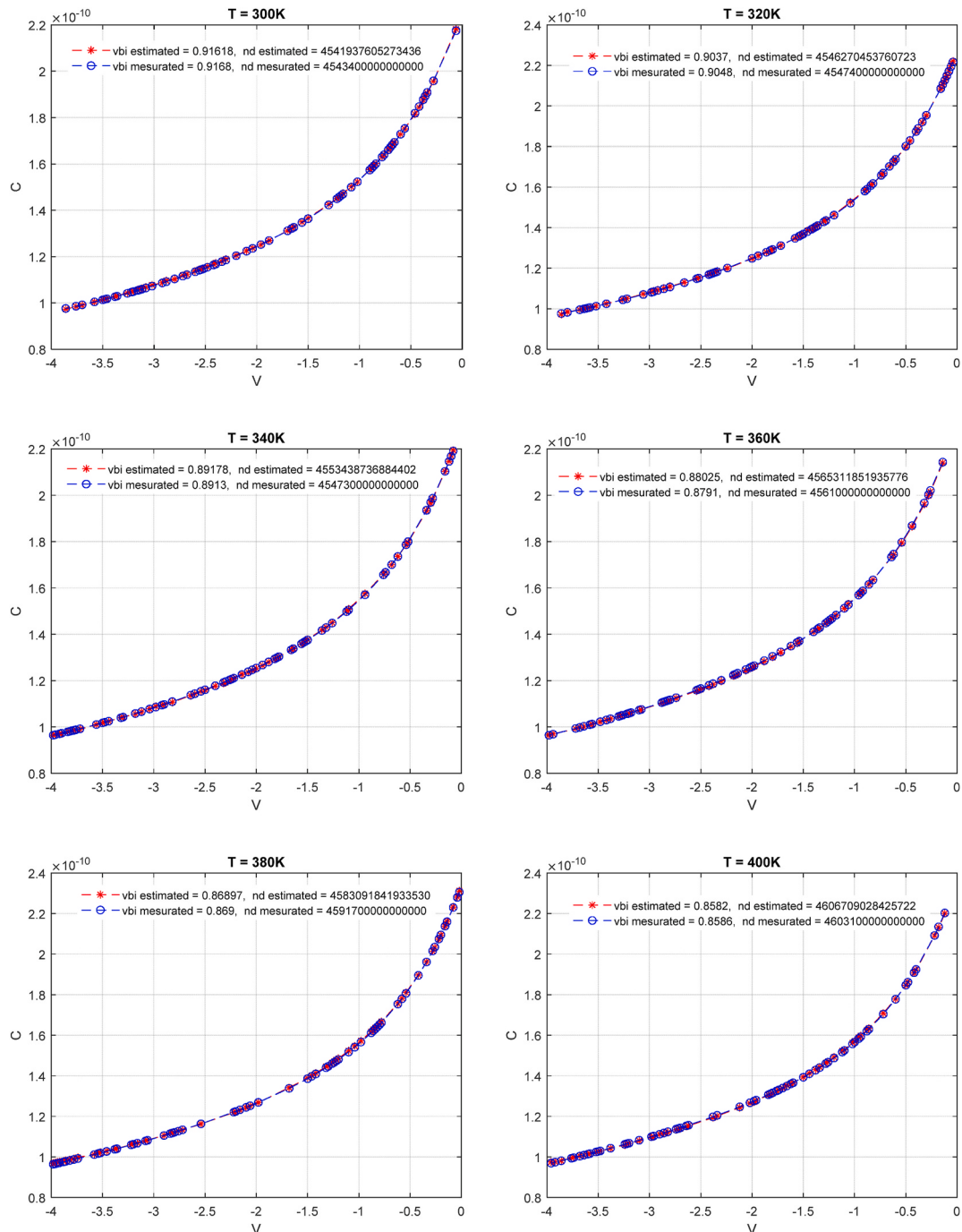


Fig. 10. (continued).

between measured and predicted values has been observed for each data set.

$R$ -values of the training, validation, testing and the entire data sets are actually quite close to one (0.9999). The slopes of regression lines are all equal to one for the training, validation, and testing data sets, and their intercepts are all very close to zero ( $2.9 \times 10^{-5}$ ,  $2.5 \times 10^{-5}$ , and 0.00014, respectively).

## 5. Conclusion

In this work, two ANN models are developed to estimate the electrical parameters of GaAs/AlGaAs MQW Schottky diodes and predict their C-V characteristics. The effectiveness of the suggested method was

evaluated through experimental measurements of capacitance in the temperature and voltage ranges of 20 K - 400 K and -4 V - 0 V, respectively. Model 1 is used to evaluate ANN's ability to predict C-V characteristics at different temperatures. Temperature and voltage are its two inputs, and capacitance is its single output. The simultaneous estimation of parameters and the C-V characteristics at various temperatures was then handled by Model 2. It has two inputs (temperature and voltage) and three outputs (capacitance, effective density, and built-in voltage). Three-fold cross-validation and mean square error are used to assess the effectiveness of the developed models. Model 1 performs an MSE of  $1.5033 \times 10^{-6}$  at 1450 epochs, while Model 2's MSE is  $4.9951 \times 10^{-6}$  at 642 epochs. As evidenced by the error distribution frequency histogram, about 95 % of errors for Models 1 and 2 fall between

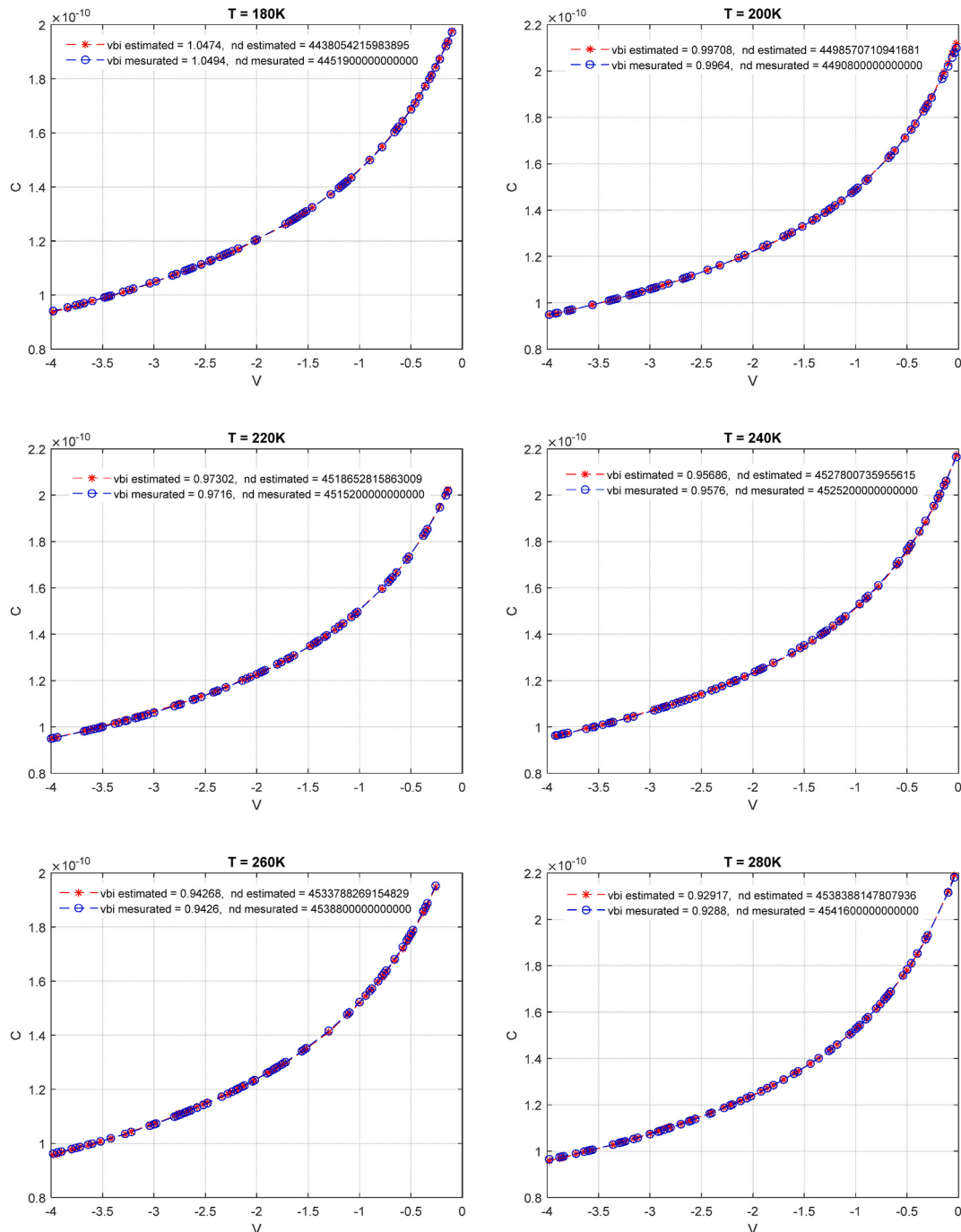
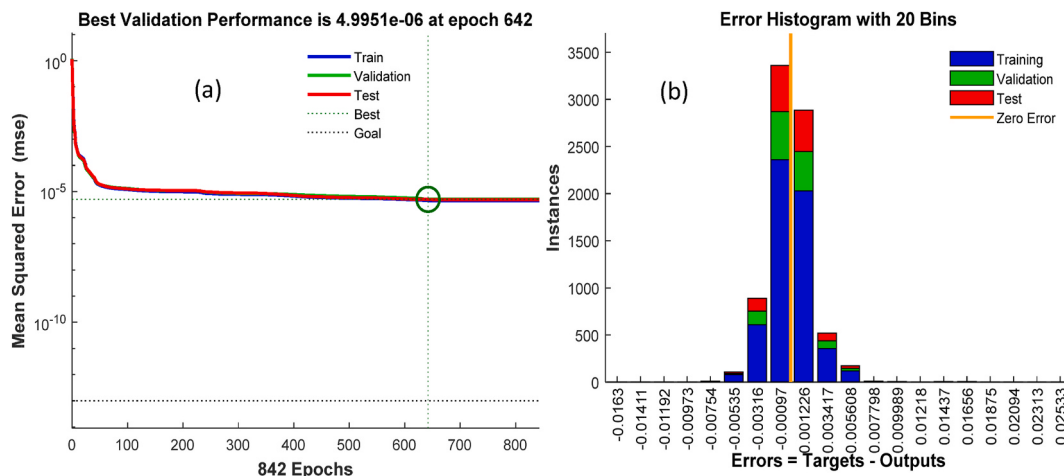


Fig. 10. (continued).

[0.00535–0.005608] and [0.00328–0.00333], respectively. Both models have R-values that are very close to one (0.9999) for the training and validation datasets. The findings of the parameter determination process utilizing Model 2 have been compared with the results obtained using the ALO-based approach. The results of the ANN models were found to be very close to the experimental data. To further verify the efficiency, correlation plots were also considered. The obtained results highlight some fascinating elements of database enrichment. It is actually possible to determine other useful electrical metrics by including I–V characteristics.

#### CRediT authorship contribution statement

**Elyes Garoudja:** Writing – original draft, Visualization, Validation, Supervision, Software, Methodology, Investigation, Formal analysis. **Assia Baouta:** Writing – review & editing, Writing – original draft, Supervision, Software, Methodology, Investigation, Formal analysis. **Abdeladhim Derbal:** Visualization, Software, Methodology. **Walid Filali:** Visualization, Validation, Supervision, Methodology, Investigation, Formal analysis. **Slimane Oussalah:** Writing – review & editing, Visualization, Validation, Supervision, Investigation. **Meriem Khelladi:** Validation, Supervision, Software. **Fouaz Lekoui:** Resources, Methodology, Investigation, Formal analysis. **Rachid Amrani:** Validation, Supervision, Methodology, Formal analysis. **Nouredine Sengouga:**



**Fig. 11.** (a) Performance evaluation of Model 2 according to epoch, (b) Error histogram of Model 2.

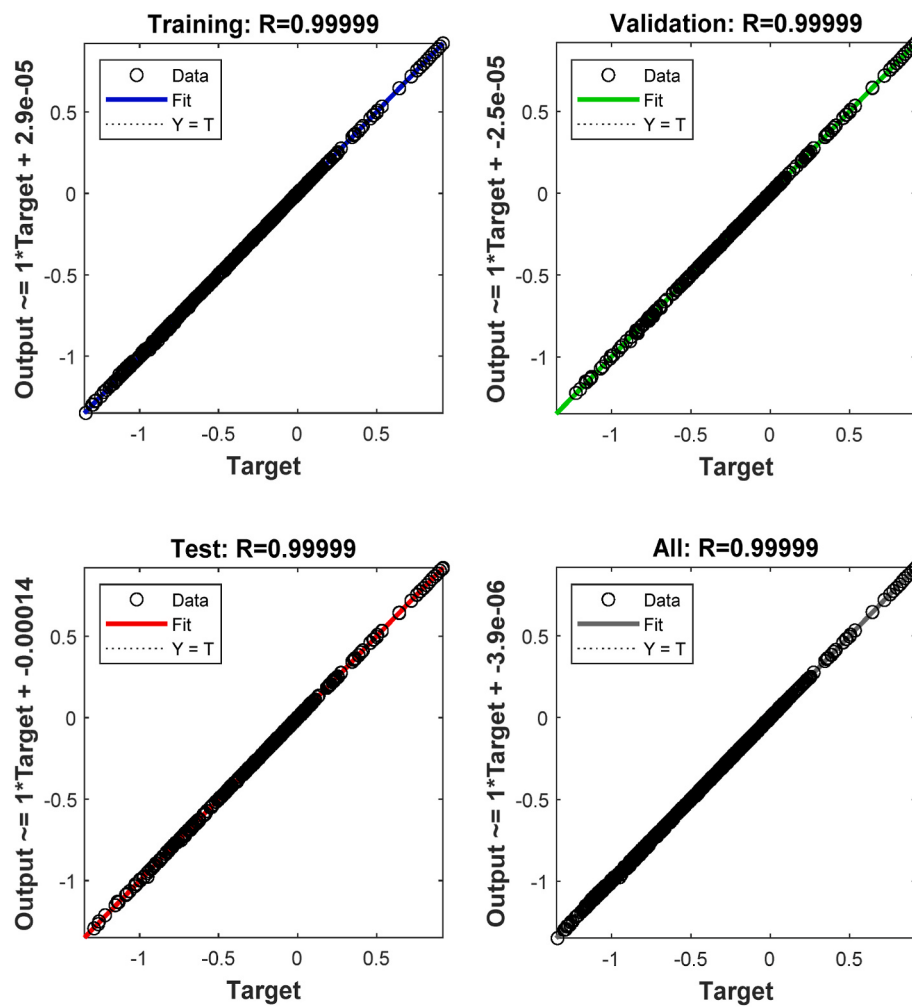


**Fig. 12.** The calculated R-values for training, validation, test and all data sets of Model 2.

Writing – review & editing, Visualization, Validation, Supervision, Investigation. **Mohamed Henini:** Validation, Supervision, Methodology, Investigation.

#### Declaration of competing interest

The authors declare that they have no known competing financial interests or personal relationships that could have appeared to influence the work reported in this paper.

## Data availability

Data will be made available on request.

## References

- [1] T. Güzel, A.B. Çolak, Artificial intelligence approach on predicting current values of polymer interface Schottky diode based on temperature and voltage: an experimental study, *Superlattice. Microst.* 153 (2021) 106864.
- [2] R. Gupta, F. Yakuphanoglu, Photoconductive Schottky diode based on Al/p-Si/SnS<sub>2</sub>/Ag for optical sensor applications, *Sol. Energy* 86 (2012) 1539–1545.
- [3] S. Ying, Z. Ma, Z. Zhou, R. Tao, K. Yan, M. Xin, Y. Li, L. Pan, Y. Shi, Device based on polymer Schottky junctions and their applications: a review, *IEEE Access* 8 (2020) 189646–189660.
- [4] W. Filali, N. Sengouga, S. Oussalah, R.H. Mari, D. Jameel, N.A. Al Saqri, M. Aziz, D. Taylor, M. Henini, Characterisation of temperature dependent parameters of multi-quantum well (MQW) Ti/Au/n-AlGaAs/n-GaAs/n-AlGaAs Schottky diodes, *Superlattice. Microst.* 111 (2017) 1010–1021.
- [5] D. Caimi, P. Tiwari, M. Sousa, K.E. Moselund, C.B. Zota, Heterogeneous integration of III–V materials by direct wafer bonding for high-performance electronics and optoelectronics, *IEEE Trans. Electron. Dev.* 68 (2021) 3149–3156.
- [6] S. Chen, W. Li, J. Wu, Q. Jiang, M. Tang, S. Shutts, S.N. Elliott, A. Sobiesierski, A. J. Seeds, I. Ross, Electrically pumped continuous-wave III–V quantum dot lasers on silicon, *Nat. Photonics* 10 (2016) 307–311.
- [7] A. Perera, Heterojunction and superlattice detectors for infrared to ultraviolet, *Prog. Quant. Electron.* 48 (2016) 1–56.
- [8] P. Pitigala, P. Jayaweera, S. Matsik, A. Perera, H. Liu, Highly sensitive GaAs/AlGaAs heterojunction bolometer, *Sens. Actuator A Phys* 167 (2011) 245–248.
- [9] E. Nazemi, S. Aithal, W.M. Hassen, E.H. Frost, J.J. Dubowski, GaAs/AlGaAs heterostructure based photonic biosensor for rapid detection of Escherichia coli in phosphate buffered saline solution, *Sensor. Actuator. B Chem.* 207 (2015) 556–562.
- [10] W. Filali, E. Garoudja, S. Oussalah, M. Mekheldi, N. Sengouga, M. Henini, A novel parameter identification approach for C–V–T characteristics of multi-quantum wells Schottky diode using ant lion optimizer, *Russ. Microelectron.* 48 (2019) 428–434.
- [11] W. Filali, R. Amrani, E. Garoudja, S. Lekou, Z. Ouikerimi, N. Sengouga, M. Henini, Optimal identification of Be-doped Al<sub>0.29</sub>Ga<sub>0.71</sub>As Schottky diode parameters using Dragonfly Algorithm: a thermal effect study, *Superlattice. Microst.* 160 (2021) 107085.
- [12] E. Garoudja, W. Filali, S. Oussalah, N. Sengouga, M. Henini, Comparative study of various methods for extraction of multi-quantum wells Schottky diode parameters, *J. Semiconduct. Technol.* 41 (2020) 102401.
- [13] S. Oussalah, W. Filali, E. Garoudja, B. Zatout, F. Lekou, R. Amrani, N. Sengouga, M. Henini, Analysis of I–VT characteristics of Be-doped AlGaAs Schottky diodes grown on (100) GaAs substrates by molecular beam epitaxy, *Microelectron. J.* 122 (2022) 105409.
- [14] S. Walczak, Artificial neural networks, in: Advanced Methodologies and Technologies in Artificial Intelligence, Computer Simulation, and Human-Computer Interaction, IGI global, 2019, pp. 40–53.
- [15] G. Wang, Y. Zhang, X. Ye, X. Mou, Artificial neural networks, in: Machine Learning for Tomographic Imaging, IOP Publishing, 2019.
- [16] M. Alade, S. Akande, G. Fajinmi, A. Adewumi, M. Alade, Prediction of the breakdown voltage of n-GaN Schottky diodes at high temperatures using online neural network analysis, *J. Eng. Appl. Sci.* 4 (2009) 114–118.
- [17] M.O. Alade, High temperature electronic properties of a microwave frequency sensor–GaN Schottky diode, *Adv. Phys. Theor. Appl.* 15 (2013) 47–53.
- [18] B. Milošević, M. Radovanović, B. Jokanović, Z. Marinković, Artificial neural network model of zero-bias Schottky diode for energy harvesting, in: 2019 14th International Conference on Advanced Technologies, Systems and Services in Telecommunications (TELSIKS), IEEE, 2019, pp. 319–322.
- [19] A. Darwish, T. Hanafy, A. Attia, D. Habashy, M. El-Bakry, M. El-Nahass, Optoelectronic performance and artificial neural networks (ANNs) modeling of n-InSe/p-Si solar cell, *Superlattice. Microst.* 83 (2015) 299–309.
- [20] A.B. Çolak, T. Güzel, O. Yıldız, M. Özer, An experimental study on determination of the shottky diode current-voltage characteristic depending on temperature with artificial neural network, *Physica B (Amsterdam, Neth.)* 608 (2021) 412852.
- [21] T. Güzel, A.B. Çolak, An experimental study on artificial intelligence-based prediction of capacitance–voltage parameters of polymer-interface 6H-SiC/MEH-PPV/Al Schottky diodes, *Phys. Status Solidi* 219 (2022) 2100821.
- [22] A.B. Çolak, T. Güzel, A. Shafiq, K. Nonlaopon, Do Artificial neural networks always provide high prediction performance? An experimental study on the insufficiency of Artificial neural networks in Capacitance Prediction of the 6H-SiC/MEH-PPV/Al Diode, *Symmetry* 14 (2022) 1511.
- [23] T. Güzel, A.B. Çolak, Investigation of the usability of machine learning algorithms in determining the specific electrical parameters of Schottky diodes, *Mater. Today Commun.* 33 (2022) 104175.
- [24] T. Güzel, A.B. Çolak, Performance prediction of current-voltage characteristics of Schottky diodes at low temperatures using artificial intelligence, *Microelectron. Reliab.* 147 (2023) 115040.
- [25] S. Cheung, N. Cheung, Extraction of Schottky diode parameters from forward current-voltage characteristics, *Appl. Phys. Lett.* 49 (1986) 85–87.
- [26] R. Fu, A.E. Grekov, K. Peng, E. Santi, Parameter extraction procedure for a physics-based power SiC Schottky diode model, *IEEE Trans. Ind. Appl.* 50 (2014) 3558–3568.
- [27] E. Garoudja, R. Amrani, W. Filali, F. Lekou, S. Oussalah, Y. Cuminal, P. Abboud, M. Henini, Artificial bee colony algorithm: a novel strategy for optical constants and thin film thickness extraction using only optical transmittance spectra for photovoltaic applications, *Optik* 241 (2021) 167030.
- [28] S. Özürk, R. Ahmad, N. Akhtar, Variants of Artificial Bee Colony algorithm and its applications in medical image processing, *Appl. Soft Comput.* 97 (2020) 106799.
- [29] A. Banharnsakun, T. Achalakul, B. Sirinaovakul, The best-so-far selection in artificial bee colony algorithm, *Appl. Soft Comput.* 11 (2011) 2888–2901.
- [30] R. Amrani, E. Garoudja, F. Lekou, W. Filali, H. Neggaz, Y.A. Djebeli, L. Henni, S. Hassani, F. Kezzoula, S. Oussalah, Investigation of structural and electrical properties of ITO thin films and correlation to optical parameters extracted using novel method based on PSO algorithm, *Bull. Mater. Sci.* 46 (2023) 8.
- [31] K.R. Opara, J. Arabas, Differential Evolution: a survey of theoretical analyses, *Swarm Evol. Comput.* 44 (2019) 546–558.
- [32] Y. Meraïhi, A. Ramdane-Cherif, D. Acheli, M. Mahseur, Dragonfly algorithm: a comprehensive review and applications, *Neural Comput. Appl.* 32 (2020) 16625–16646.
- [33] V.R. Vc, Ant Lion optimization algorithm for optimal sizing of renewable energy resources for loss reduction in distribution systems, *J. Electr. Syst. Inf. Technol* 5 (2018) 663–680.
- [34] S.M. Sze, Y. Li, K.K. Ng, Physics of Semiconductor Devices, John Wiley & Sons, 2021.
- [35] H. Norde, A modified forward I–V plot for Schottky diodes with high series resistance, *J. Appl. Phys.* 50 (1979) 5052–5053.
- [36] A. Abraham, Artificial Neural Networks, *Handbook of Measuring System Design*, 2005.
- [37] D. Graupe, Principles of Artificial Neural Networks, World Scientific, 2013.
- [38] I. Hovden, Optimizing Artificial Neural Network Hyperparameters and Architecture, University of Oslo, Oslo, 2019.
- [39] P.R. Lorenzo, J. Nalepa, M. Kawulok, L.S. Ramos, J.R. Pastor, Particle swarm optimization for hyper-parameter selection in deep neural networks, in: Proceedings of the Genetic and Evolutionary Computation Conference, 2017, pp. 481–488.
- [40] X. Yao, Y. Liu, Towards designing artificial neural networks by evolution, *Appl. Math. Comput.* 91 (1998) 83–90.
- [41] S. Mirjalili, The ant lion optimizer, *Adv. Eng. Software* 83 (2015) 80–98.
- [42] T. Fushiki, Estimation of prediction error by using K-fold cross-validation, *Stat. Comput.* 21 (2011) 137–146.